Electromagnetic modeling for SAR polarimetry and interferometry

PhD candidate:
Davod Poreh

Tutor:
Prof. Daniele Riccio

My PHD details

- **Fellowship** – From Universita degli Studi di Napoli Federico II (three years)

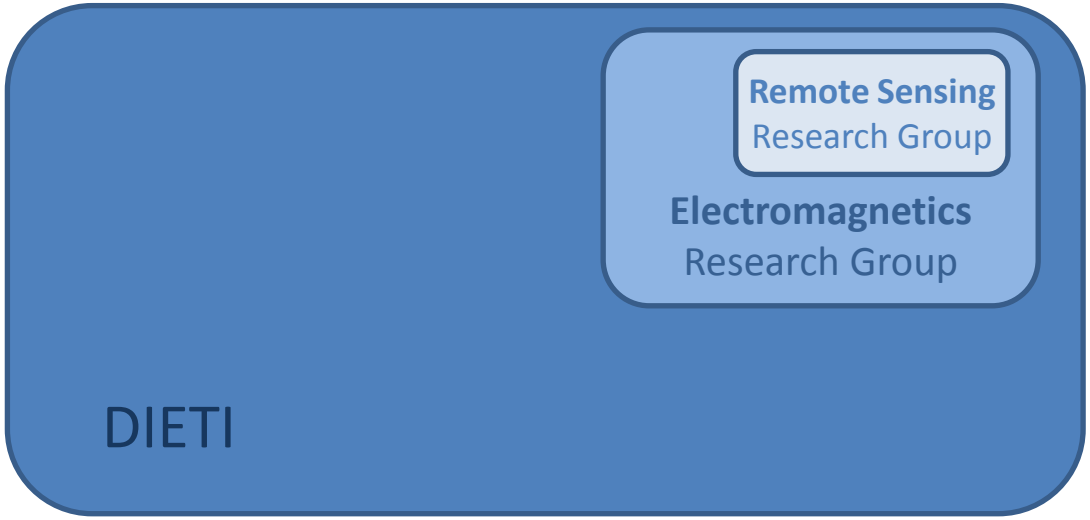

My personal data for Ph.D.

- Training activities:

	Credits year 1									Credits year 2									Credits year 3									
		1	2	3	4	5	6				1	2	3	4	5	6				1	2	3	4	5	6			
	Estimated	bimonth	bimonth	bimonth	bimonth	bimonth	bimonth	Sum	Check	Estimated	bimonth	bimonth	bimonth	bimonth	bimonth	bimonth	Sum	Check	Estimated	bimonth	bimonth	bimonth	bimonth	bimonth	bimonth	Sum	Check	Total
Modules	20	0	0	0	9	9	3	21	20-40	10	6	6	3	0	0	0	15	10-20	0	0	3	0	0	0	3	6	0-10	42
Seminars	5	0	1.1	1.9	0.4	0.5	0.2	4.1	5-10	5	0.6	0.5	0.2	0	0	0	1.3	5-10	0	0	0	0	0	0	1	1	0-10	6.4
Research	30	10	8.9	8.1	0.6	0.5	6.8	35	10-35	40	3.4	3.5	6.8	10	10	10	44	30-45	60	10	7	10	10	10	6	53	40-60	131.6
	55	10	10	10	10	10	10	60		55	10	10	10	10	10	10	60		60	10	10	10	10	10	10	60		180

Year	Course	Credits
1	Multivariate image processing II	9
1	Radio coverage for signal networks	9
1	Designing and writing scientific manuscript for publication in English language scholarly journals	3
2	Radar systems	6
2	Mathematical foundation of filed computation and magnetic measurements for accelerator magnets	3
2	Using satellite radar for infrastructure health monitoring	3
2	Scientific writing	3
3	Satellite Remote Sensing: Open challenges and opportunities	3
3	Introduction to Quantum Electrodynamics	3
Total		42

Year	Seminar	Credits
1	Applications for software development: types, interactions and continuous integration	0.5
1	Mechanics of Solids: From beam theory to rapid prototyping for surgery planning	0.2
1	Risk management meets model checking: fault tree analysis and model-based testing via games	0.4
1	Reliability of dispositive and electronic forms of power	1.1
1	The iCub project: an open platform for research in robotic& artificial intelligent	0.3
1	Partial possibilistic regression path modeling	0.5
1	Passivity-base control of nonlinear physical systems: A port Hamilton approach	0.4
1	Lecture on current and future trends in advance antenna application	0.5
1	On the complexity of temporal equilibrium logic (joint work with David Pearce)	0.2
2	CMOS smart gas sensors, temperature sensors and IR devices	0.6
2	Radar adaptively: Antenna based signal processing technique	0.5
2	GIELIS transformations in the natural sciences and technology	0.2
3	Radar and SAR systems for airborne and space-based surveillance and reconnaissance	1.0
Total		6.4

Outline

PART I

- ✓ **Railways' stabilities observed/modelled in Campania (Italy) by InSAR data**
- ✓ **Principles of InSAR and PSI**
- ✓ **Data, and data analysis**
- ✓ **Conclusions**

PART II

- ✓ **A fully polarimetric SAR raw signal simulator**
- ✓ **Polarimetirc simulation rationale**
- ✓ **Simulation results**
- ✓ **Conclusions**

Outline

PART I

- ✓ **Railways' stabilities observed/modelled in Campania (Italy) by InSAR data**
- ✓ **Principles of InSAR and PSI**
- ✓ **Data, and data analysis**
- ✓ **Conclusions**

PART II

- ✓ **A fully polarimetric SAR raw signal simulator**
- ✓ **Polarimetirc simulation rationale**
- ✓ **Simulation results**
- ✓ **Conclusions**

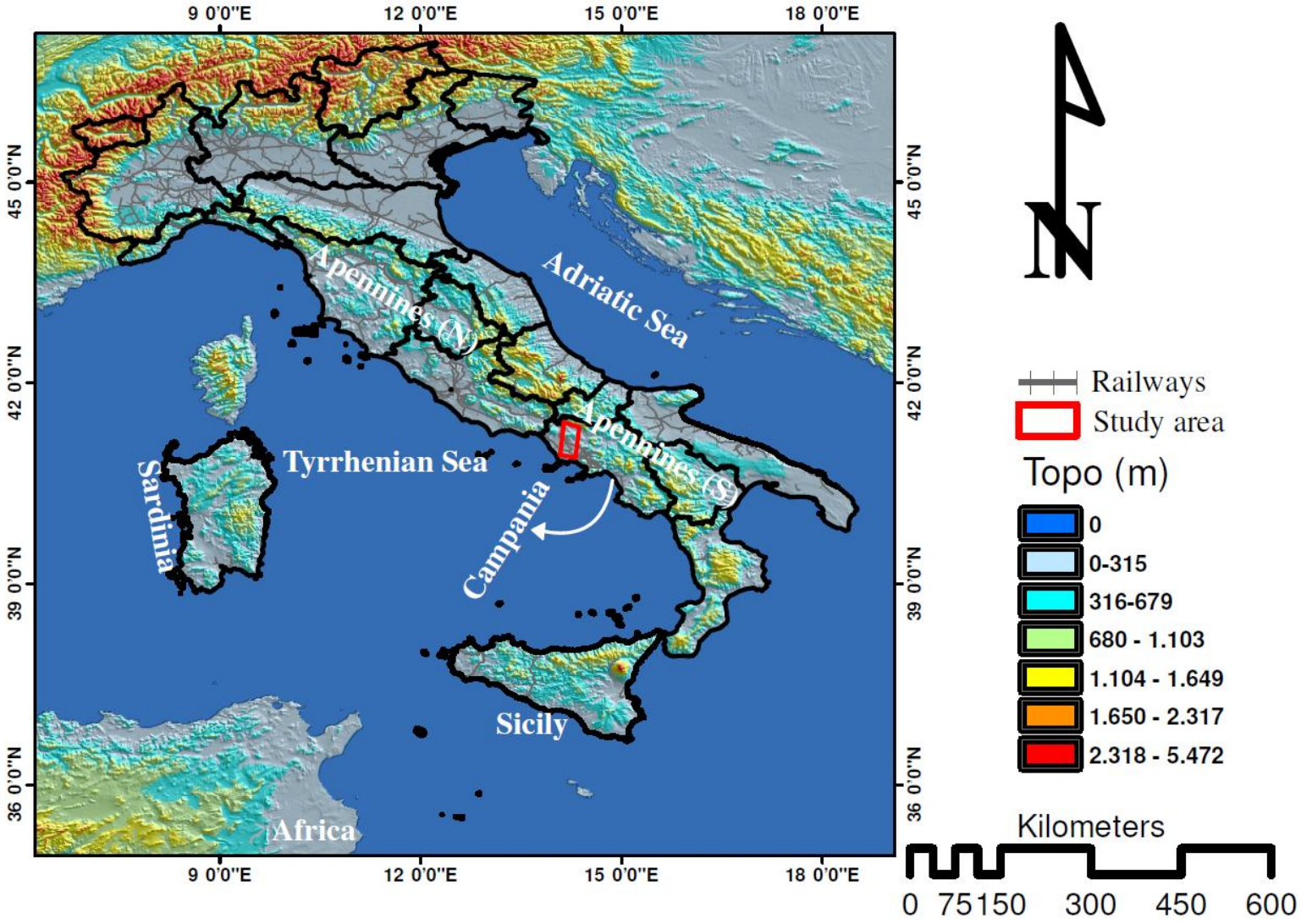

- **Intense urbanization**, active **volcanoes**, complicated **fault** systems, **landslides**, **subsidence**, and hydrological instability (**flooding**),

- 246 out of 652 **sinkholes** (38%) of entire Italy.

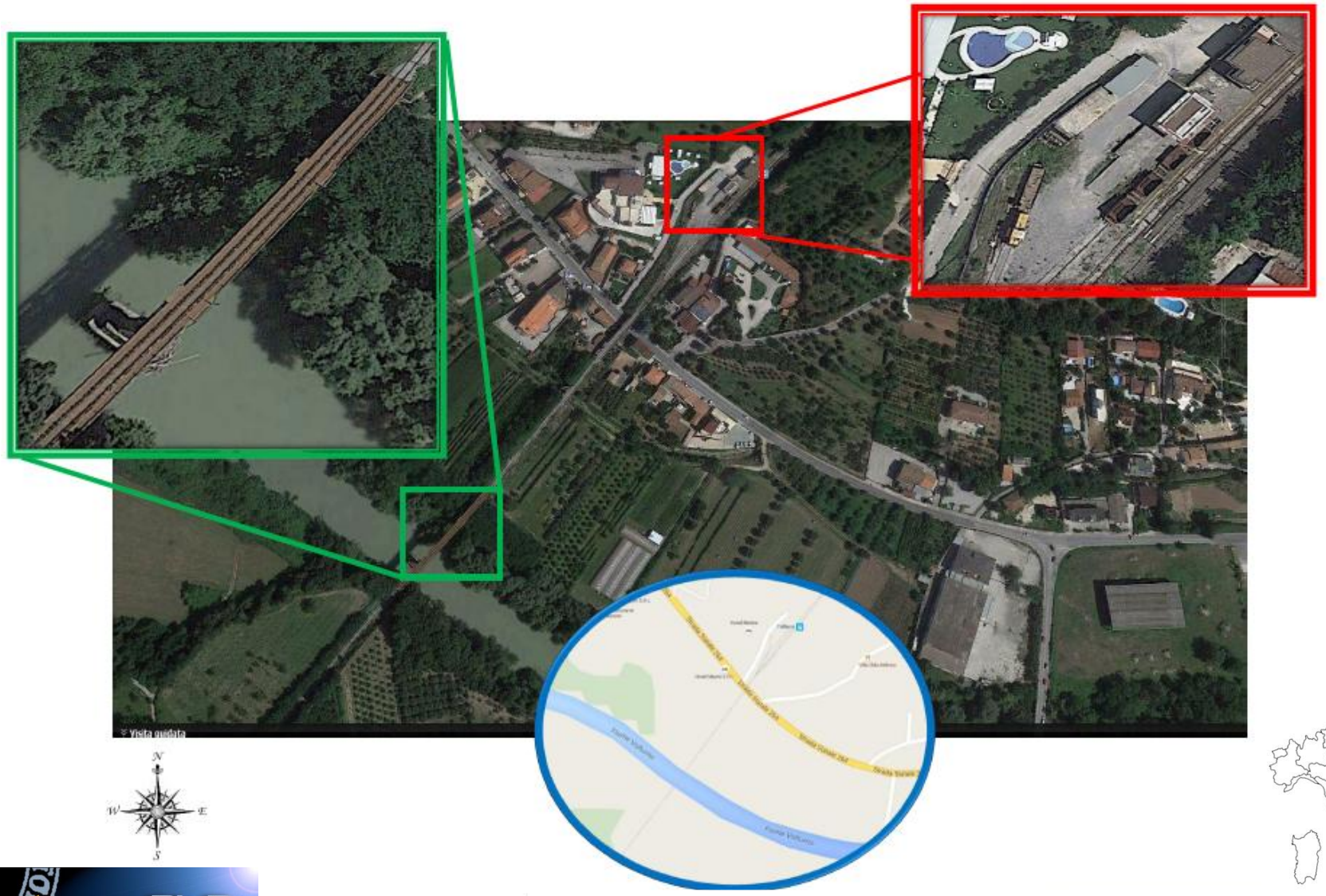
Visita guidata


Campania

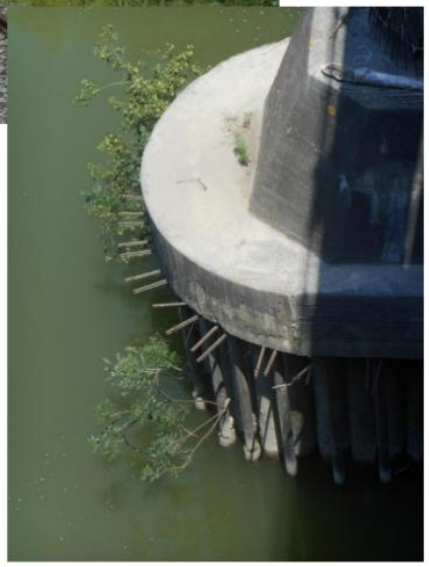

Sul versante ovest il pilone è sgrombro.
All'estremità sud del ponte è presente un traliccio e un sovrapassaggio stradale

Outline

PART I

- ✓ Railways' stabilities observed/modelled in Campania (Italy) by InSAR data
- ✓ **Principles of InSAR and PSI**
- ✓ Data, and data analysis
- ✓ Conclusions

PART II

- ✓ A fully polarimetric SAR raw signal simulator
- ✓ Polarimetirc simulation rationale
- ✓ Simulation results
- ✓ Conclusions

Persistent Scatterer (PS)

- Conventional interferometric synthetic aperture radar (InSAR) is a very effective technique for measuring crustal deformation, BUT
- Almost any interferogram includes large areas where the signals decorrelate and no measurement is possible. Persistent scatterer (PS) InSAR overcomes the decorrelation problem by identifying resolution elements whose echo is dominated by a single scatterer in a series of interferograms.
- PSI methods have been very successful in analysis of urban areas.
- Coverage of large area (100*100 km^2). GPS – Leveling
- May NOT work in rural areas, or where deformation is irregular in time.

Outline

PART I

- ✓ Railways' stabilities observed/modelled in Campania (Italy) by InSAR data
- ✓ Principles of InSAR and PSI
- ✓ **Data, and data analysis**
- ✓ Conclusions

PART II

- ✓ A fully polarimetric SAR raw signal simulator
- ✓ Polarimetirc simulation rationale
- ✓ Simulation results
- ✓ Conclusions

- ✓ **25 CosmoSkyMed images from 2011 until 2015.**
- ✓ **One point on the bridge has been selected as a central point, and images were cropped in an area like 7.5*7.5 km^2**
- ✓ **24 interferograms have been calculated with respect to image 20130605.**
- ✓ **193k PSs have been generated.**
- ✓ **On the bridge 30 PSs selected.**

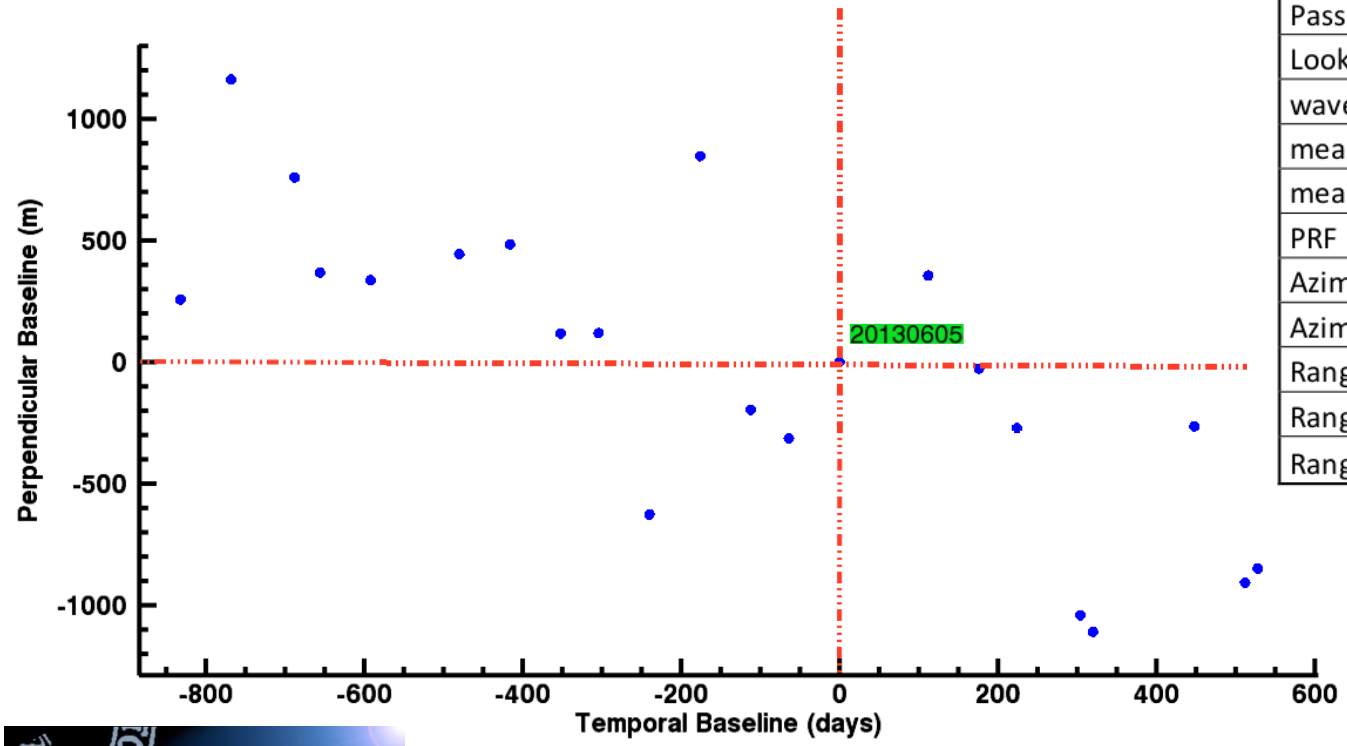

Description [unit]	Value
Mode	Stripmap
Polarization	HH
Pass	Descending
Look Side	Right
wavelength [m]	0.031228
meanrangedistance [m]	694658.7989
meanincidangle [deg]	26.6055
PRF [Hz]	3135.4515
AzimuthBandwidth [Hz]	2633.7793
AzimuthSpacing [m]	2.2069
RangeSamplingRate [MHz]	161.25
RangeBandWidth [MHz]	132.2754
RangeSpacing [m]	0.92959

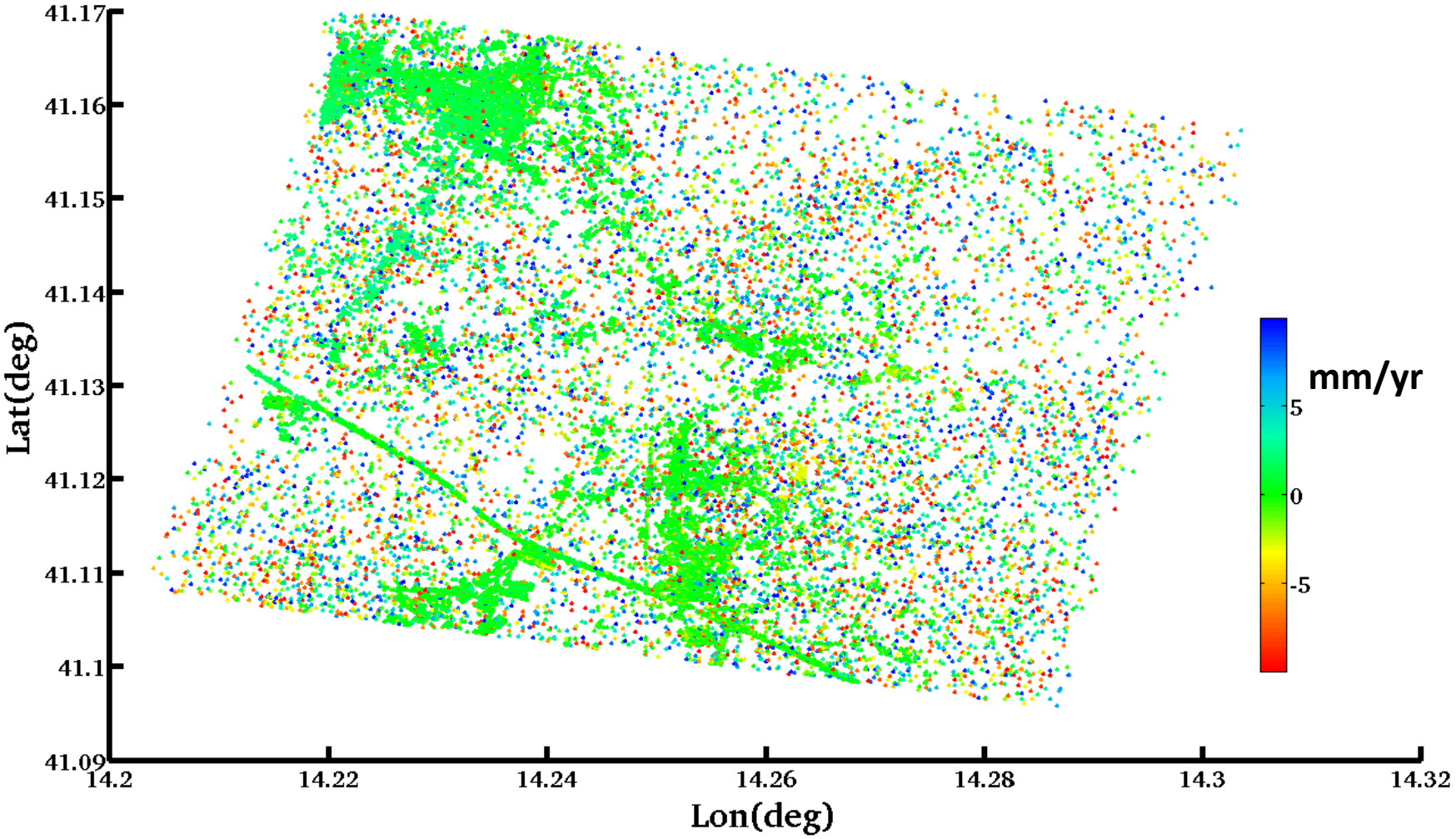
41.17
41.16
41.15
41.14
41.13
41.12
41.11
41.1
41.09
Lat(deg)
14.2
14.22
14.24
14.26
14.28
14.3
14.32
Lon(deg)
mm/yr
5
0
-5

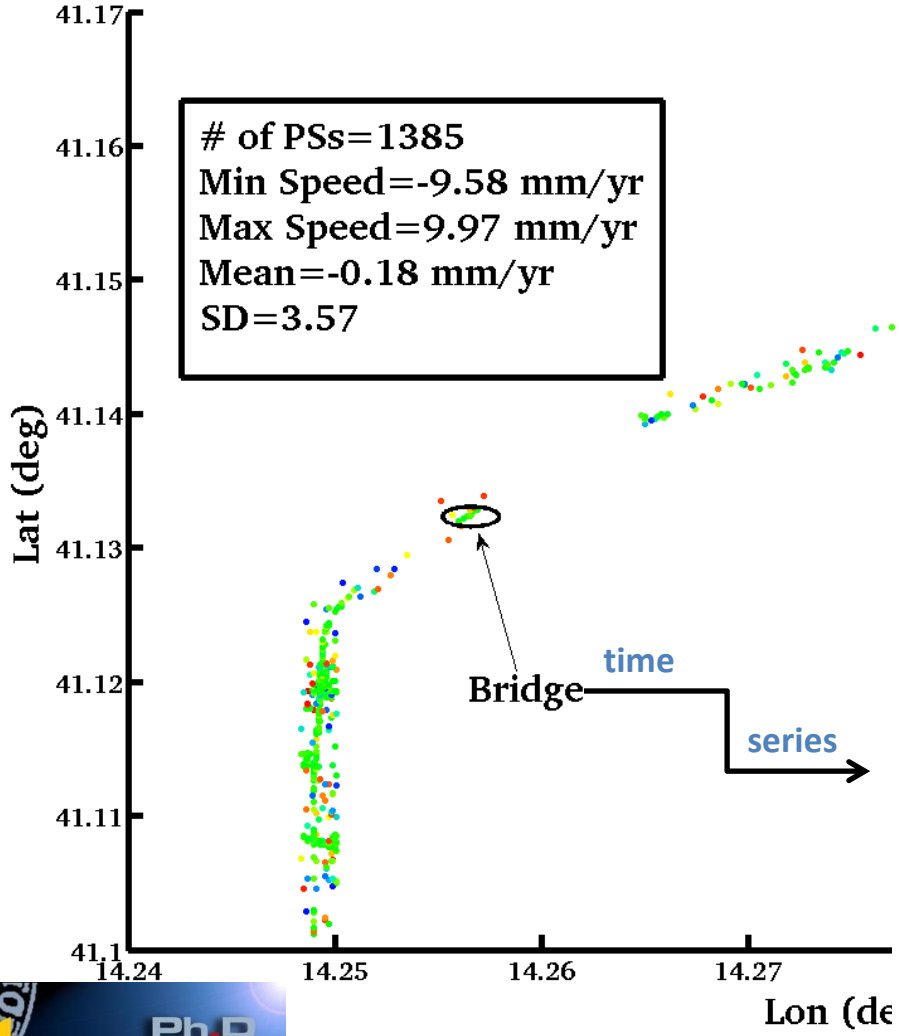
# of PSs=1385
Min Speed=-9.58 mm/yr
Max Speed=9.97 mm/yr
Mean=-0.18 mm/yr
SD=3.57
Lat (deg)
41.17
41.16
41.15
41.14
41.13
41.12
41.11
41.1
14.24
14.25
14.26
14.27
Lon (de
Bridge
time
series

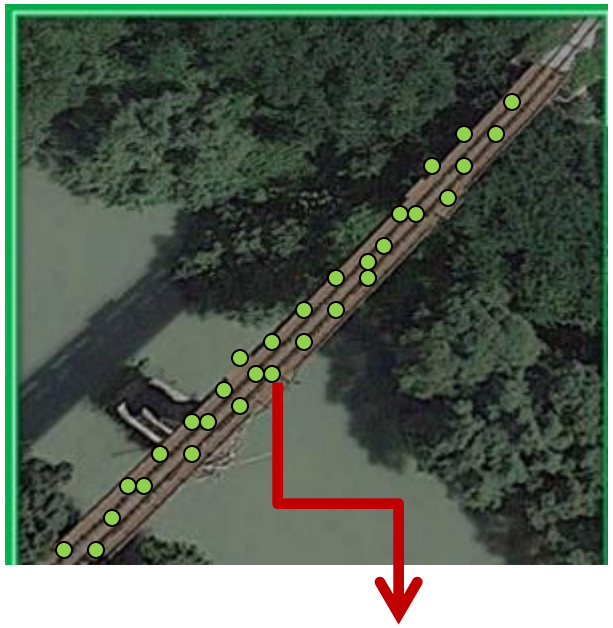

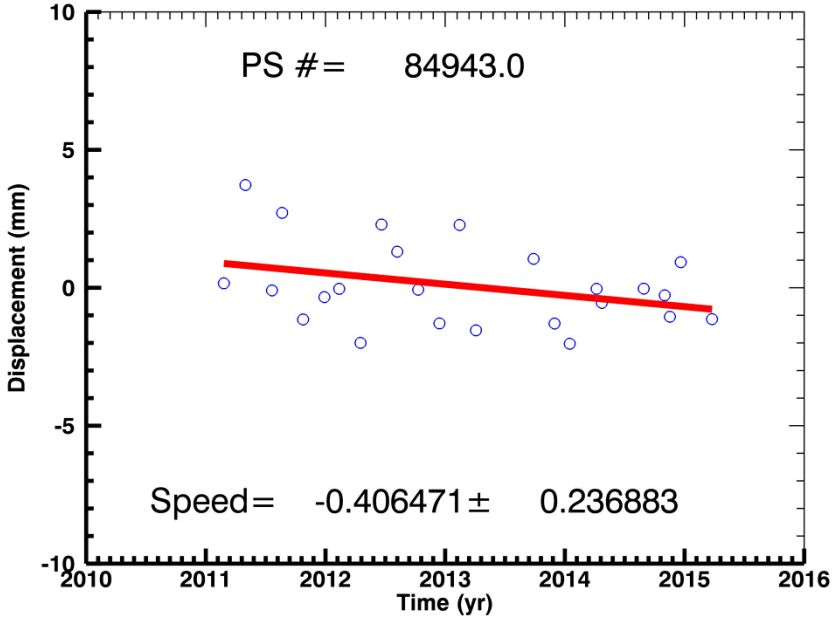
PS #= 84943.0
Displacement (mm)
10
5
0
-5
-10
2010
2011
2012
2013
2014
2015
2016
Time (yr)
Speed= -0.406471± 0.236883

PSI & Temperature

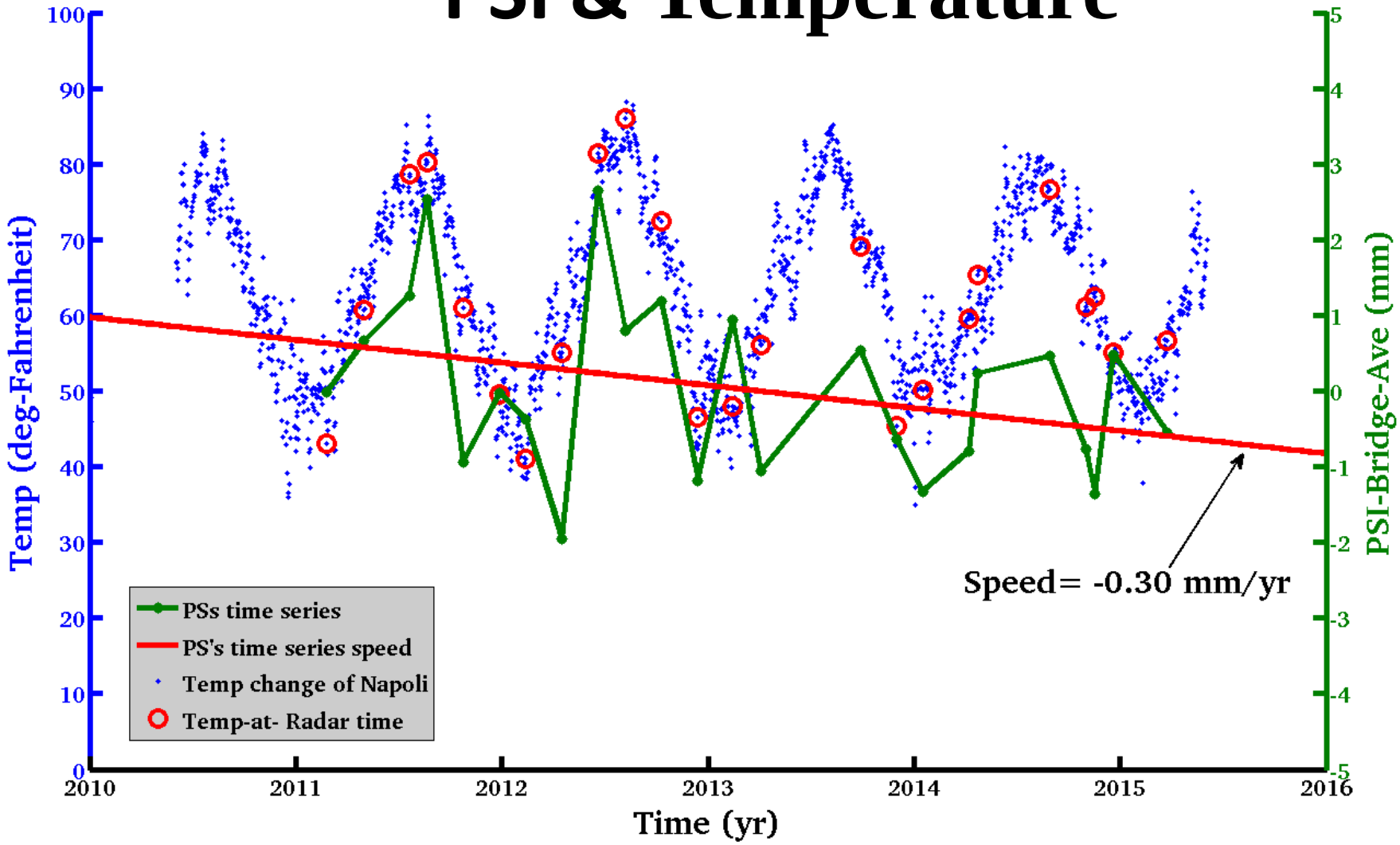

Temp data is From NOAA:
http://www7.ncdc.noaa.gov/CDO/cdoselect.cmd?datasetabbv=GSOD&countryabbv=&georegionabbv=

Outline

PART I

- ✓ Railways' stabilities observed/modelled in Campania (Italy) by InSAR data
- ✓ Data, and data analysis
- ✓ **Conclusions**

PART II

- ✓ A fully polarimetric SAR raw signal simulator
- ✓ Polarimetirc simulation rationale
- ✓ Simulation results
- ✓ Conclusions

Conclusions

- **We analyzed 25 X-band radar images of CosmoSkyMed satellite from Campania (Italy), with InSAR and PSI methodologies.**
- **In the average of more than 190 thousands of persistent scatterers, velocities, and ensemble coherence are as big as -1.8 mm/yr, and 73% respectively.**
- **On the bridge over the Volturno river (the main target), 30 PSs have been selected. In the studied time series, minimum velocity of -0.9 and maximum of 0.05 mm/yr with average of -0.3 mm/yr and SD=0.3 mm/yr has been observed, demonstrating the very stable condition on the bridge.**
- **Comparison of average PSs time series on the bridge with thermal data shows that most of the Line Of Sight (LOS) changes are due to the periodical variations of temperature (i.e., winter and summer).**

Outline

PART I

- ✓ Railways' stabilities observed/modelled in Campania (Italy) by InSAR data
- ✓ Principles of InSAR and PSI
- ✓ Data, and data analysis
- ✓ Conclusions

PART II

- ✓ **A fully polarimetric SAR raw signal simulator**
- ✓ Polarimetirc simulation rationale
- ✓ Simulation results
- ✓ Conclusions

✓ We present a new Synthetic Aperture Radar (SAR) raw signal simulator, which is able to simultaneously generate the **raw** signals of the different polarimetric channels of a polarimetric SAR system in such a way that the **correct covariance matrix** is obtained for the final images. Extended natural scenes, dominated by **surface** scattering, are considered.

✓ Synthetic Aperture Radar (SAR) Polarimetry has been successfully applied to **soil moisture retrieval**, **forest monitoring**, **change detection** and **marine applications** …

✓ Polarimetric SAR raw signal simulator, based on a sound physical electromagnetic scattering model, would be certainly useful for **mission planning**, **algorithm development and testing**, and **prediction of suitability** of the system to different applications.

✓ Simulated raw signals of the different polarimetric channels, when focused via standard SAR processing algorithms, should lead to a **realistic** polarimetric covariance (or coherency) matrix.

✓ Pol-SARAS, is made on the much older well-known SARAS [1-2] simulator, a **model-based** raw signal simulator, which also accounts for the transmitting and receiving **polarizations**.

✓ SARAS simulates **only one** polarimetric channel at a time, with the result that data of different channels turn out to be **independent**. Despite the correct relations between polarimetric channels' powers, the covariance matrix of the final images is **not realistic** (it is diagonal).

✓ The new version of SARAS simulator is able to simultaneously produce the raw signals of the different polarimetric channels in such a way as to obtain the correct covariance or coherence matrixes on the final images/channels.

[1] G. Franceschetti, M. Migliaccio, D. Riccio, and G. Schirinzi, "SARAS: a synthetic aperture radar (SAR) raw signal simulator", *IEEE Trans. Geosc. Remote Sens.*, vol. 30, no. 1, pp.110-123, Jan. 1992.
[2] S. Cimmino, G. Franceschetti, A. Iodice, D. Riccio, and G. Ruello, "Efficient Spotlight SAR Raw Signal Simulation of Extended Scenes", *IEEE Trans. Geosc. Remote Sens.*, vol. 41, no. 10, pp. 2329- 2337, Oct. 2003.

Outline

PART I

- ✓ Railways' stabilities observed/modelled in Campania (Italy) by InSAR data
- ✓ Principles of InSAR and PSI
- ✓ Data, and data analysis
- ✓ Conclusions

PART II

- ✓ A fully polarimetric SAR raw signal simulator
- ✓ **Polarimetirc simulation rationale**
- ✓ Simulation results
- ✓ Conclusions

- The surface macroscopic height profile is approximated by rectangular rough facets, large with respect to wavelength but smaller than SAR system resolution.

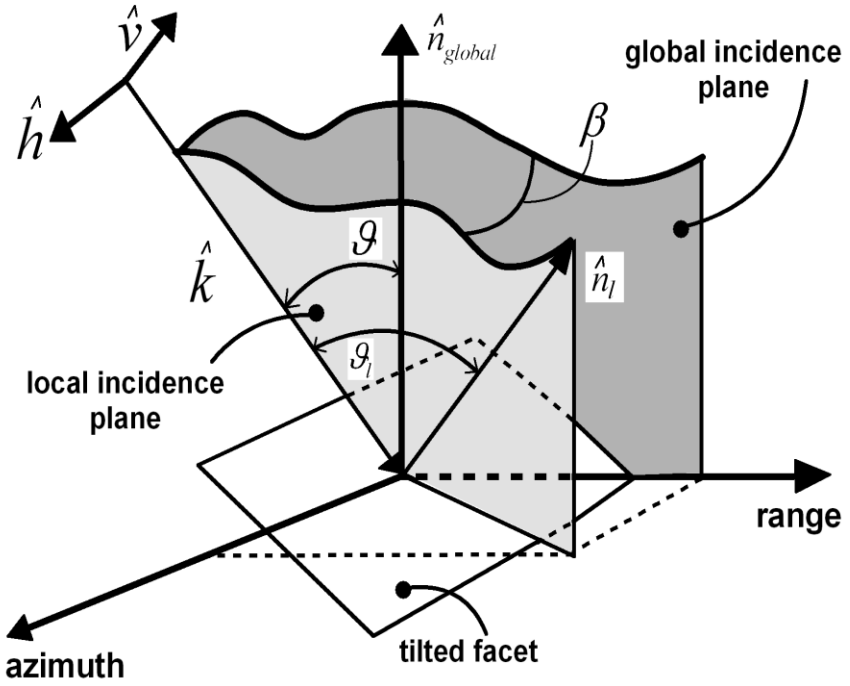

Simulator Input

***Scene data*:** height profile, Small-scale and large-scale roughness, permittivity map

***Illumination data*:** sensor height, scene-center look angle, and carrier frequency

***System data*:** sensor velocity, antenna size, chirp bandwidth and duration, pulse repetition frequency (PRF), and received pulse sampling frequency.

- Facet roughness is modelled as a stochastic process,
- Zero-mean band-limited ***2D*** fractional Brownian motion (***fBm***)

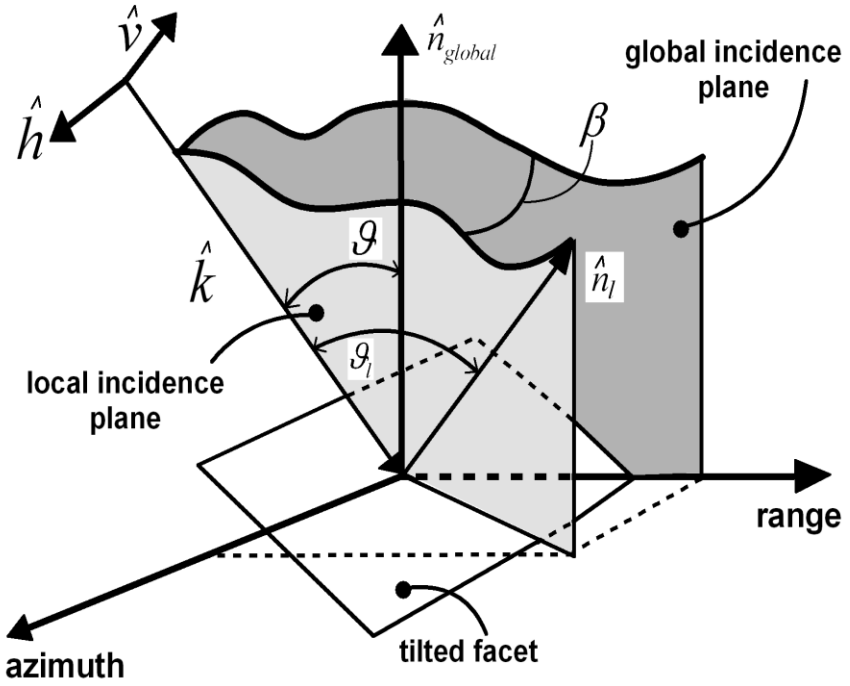

Simulator Input

***Scene data*:** height profile- Small-scale, and large-scale roughness-permittivity map

***Illumination data*:** sensor height, scene-center look angle, and carrier frequency

***System data*:** sensor velocity, antenna size, chirp bandwidth and duration, pulse repetition frequency (PRF) and received pulse sampling frequency.

$a = a_0 + \delta a$

$b = b_0 + \delta b$

r.v.

Slope from DEM

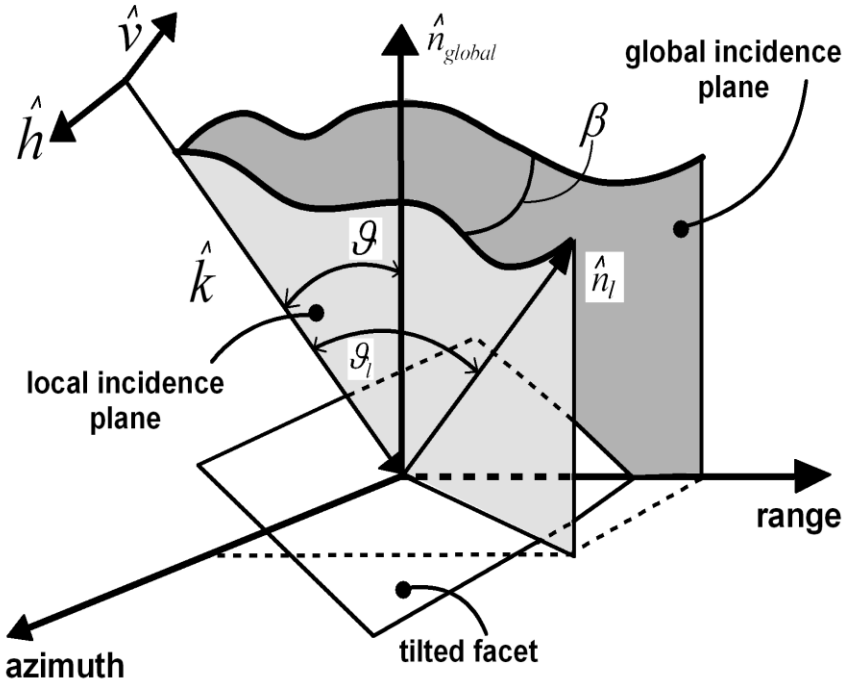

• **Zero-mean <u>random</u> deviations of the facets' azimuth and range slopes:**

$$p(\delta a, \delta b) = \frac{1}{2\pi\sigma_x\sigma_y\sqrt{1-\rho^2}} exp\left[-\frac{1}{1-\rho^2}\left(\frac{\delta a^2}{2\sigma_x^2} + \frac{\delta b^2}{2\sigma_y^2} - \frac{\rho\delta a\delta b}{\sigma_x\sigma_y}\right)\right]$$

- **Computation of <u>reflectivity map</u>**
- **<u>Superposition</u> integral**

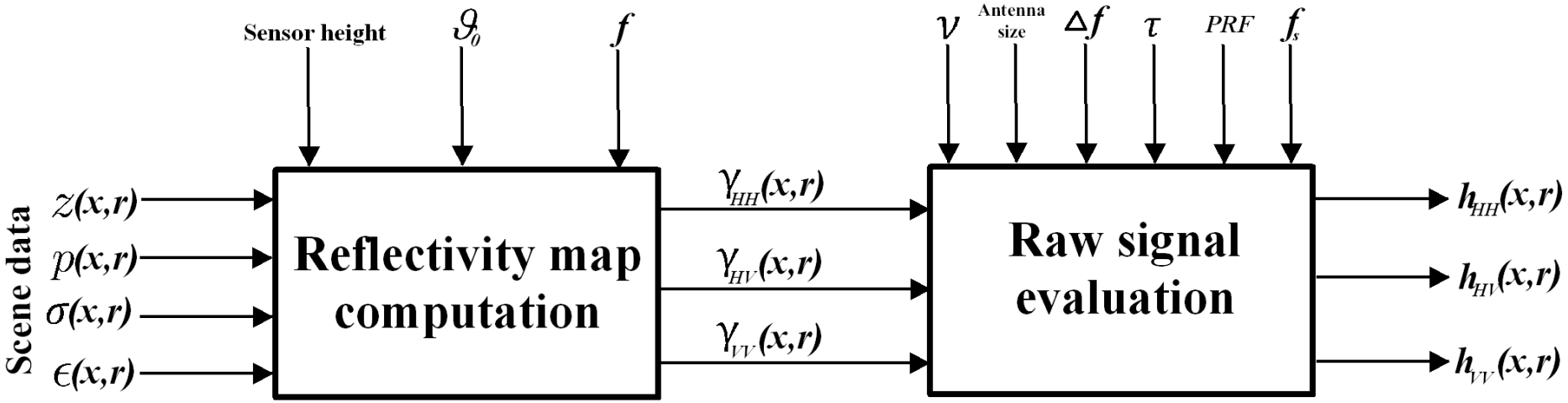

$$h_{pq}(x',r') = \iint \gamma_{pq}(x,r)\, g(x'-x, r'-r; r)\, dx\, dr$$

- ***v: sensor velocity***
- ***Δf : bandwidth***
- ***τ : pulse duration***
- ***PRF: pulse repetation frequency***
- ***f_s : pulse sampling frequency***
- ***g(.): system impulse response***

- *z(x,y): macroscopic height profile*
- *p(x,y): small-scale roughness maps*
- ϑ_0 *: scene center look angle*
- *f: carrier frequency*

- ***Reflectivity of each facet: SPM and/or PO***
- ***SPM : low roughness & intermediate incidence angles***
- ***PO: high roughness or small incidence angles***

$$\gamma_{pq}(x, r; \vartheta_l, \beta, \epsilon) = \chi_{pq}(x, r, \vartheta_l, \beta, \epsilon) w(x, r; \vartheta_l)$$

$$\underline{\underline{\chi}}(\vartheta_l, \beta, \epsilon) = \underline{\underline{R}}_2(\beta) \begin{pmatrix} F_H(\vartheta_l, \epsilon) & 0 \\ 0 & F_V(\vartheta_l, \epsilon) \end{pmatrix} \underline{\underline{R}}_2^{-1}(\beta)$$

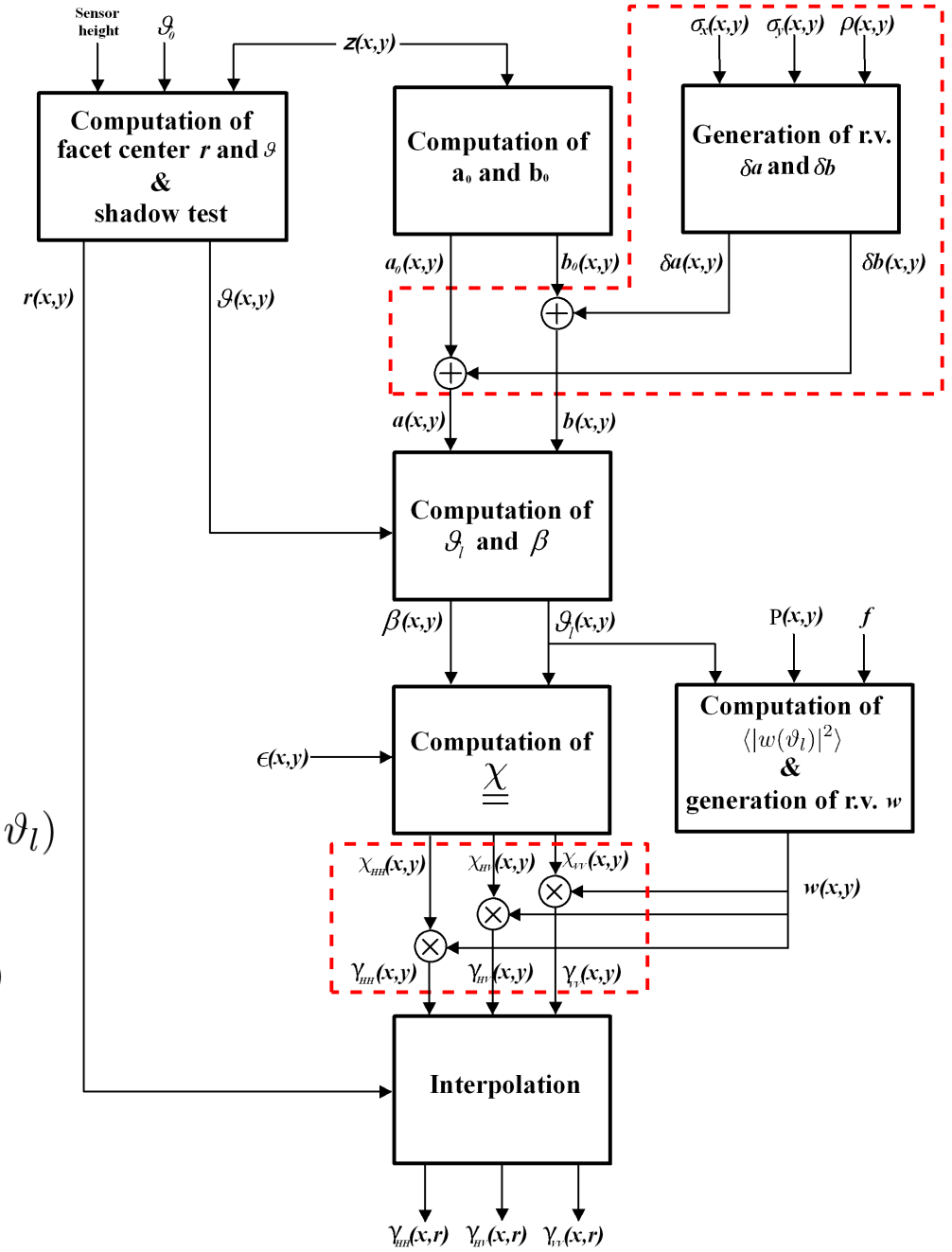

Outline

PART I

- ✓ Railways' stabilities observed/modelled in Campania (Italy) by InSAR data
- ✓ Principles of InSAR and PSI
- ✓ Data, and data analysis
- ✓ Conclusions

PART II

- ✓ A fully polarimetric SAR raw signal simulator
- ✓ Polarimetirc simulation rationale
- ✓ **Simulation results**
- ✓ Conclusions

A. Comparison with theoretical models

PTSM [3], and X-Bragg [4] with Pol-SARAS

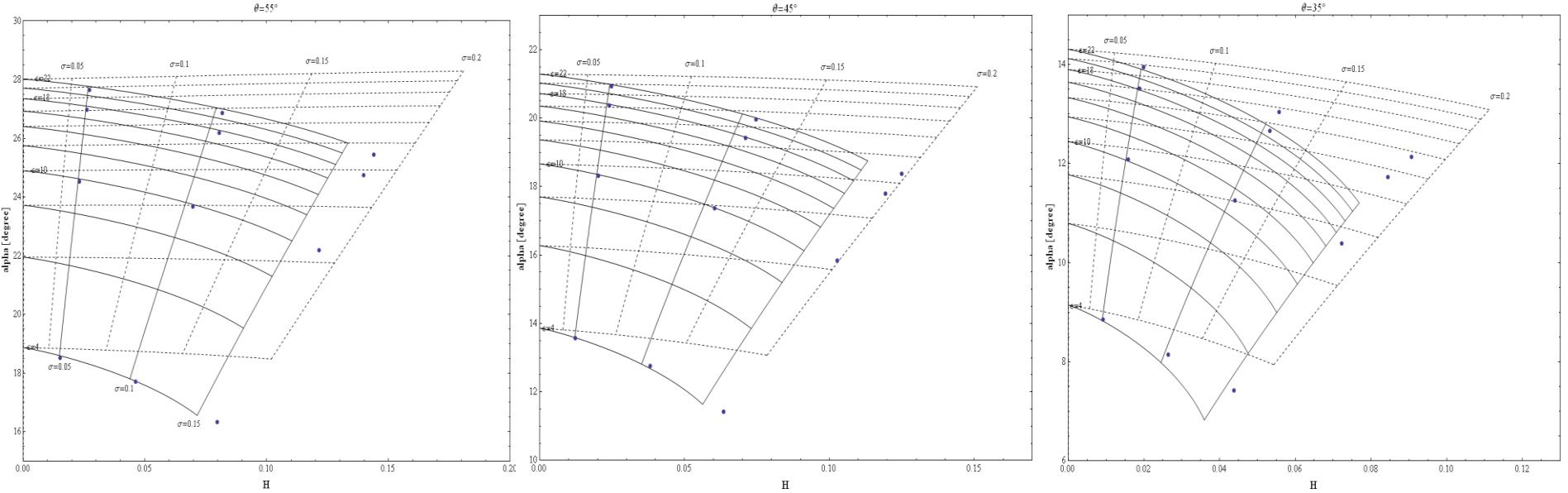

Pol-SARAS points are evaluated for **ε** equal to 4, 10, 18, and 22, and for **σ** equal to 0.05, 0.1, and 0.15.

[3] A. Iodice, A. Natale, and D. Riccio, "Retrieval of Soil Surface Parameters via a Polarimetric Two-Scale Model", *IEEE Trans. Geosc. Remote Sens.*, vol. 49, no. 7, pp. 2531-2547, July 2011.

[4] I. Hajnsek, E. Pottier, and S. R. Cloude, "Inversion of surface parameters from polarimetric SAR," *IEEE Trans. Geosci. Remote Sens.*, vol. 41, no. 4, pp. 727–744, Apr. 2003.

B. Simulation with flat surfaces

Copol-crosspol/Copol-corr graphs for different incident angles

$$\begin{cases} copol = \dfrac{\langle |i_{HH}|^2 \rangle}{\langle |i_{VV}|^2 \rangle} \\ crosspol = \dfrac{\langle |i_{HV}|^2 \rangle}{\langle |i_{VV}|^2 \rangle} \\ corr = \dfrac{|\langle i_{HH} i_{VV}^* \rangle|}{\sqrt{\langle |i_{HH}|^2 \rangle \langle |i_{VV}|^2 \rangle}} \end{cases}$$

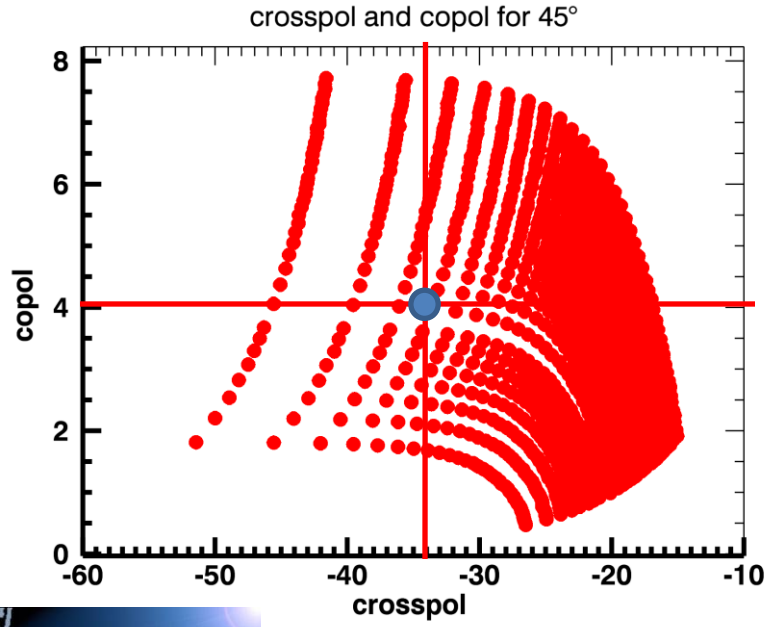

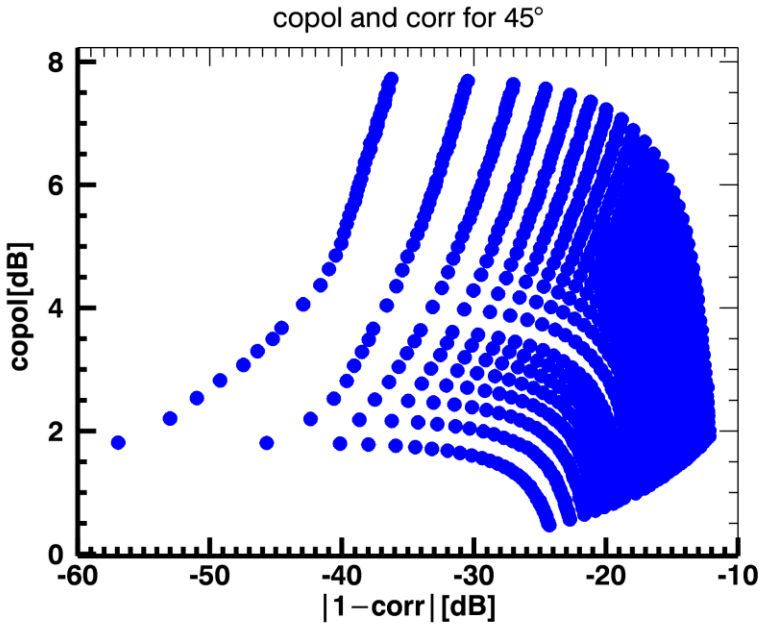

C. Anisotropic soil roughness

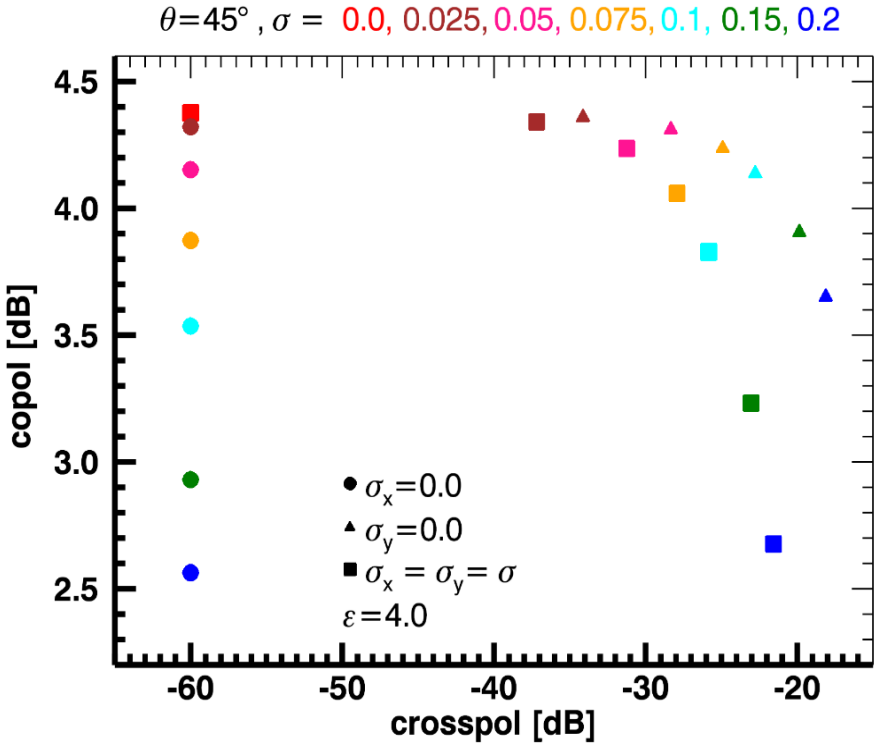

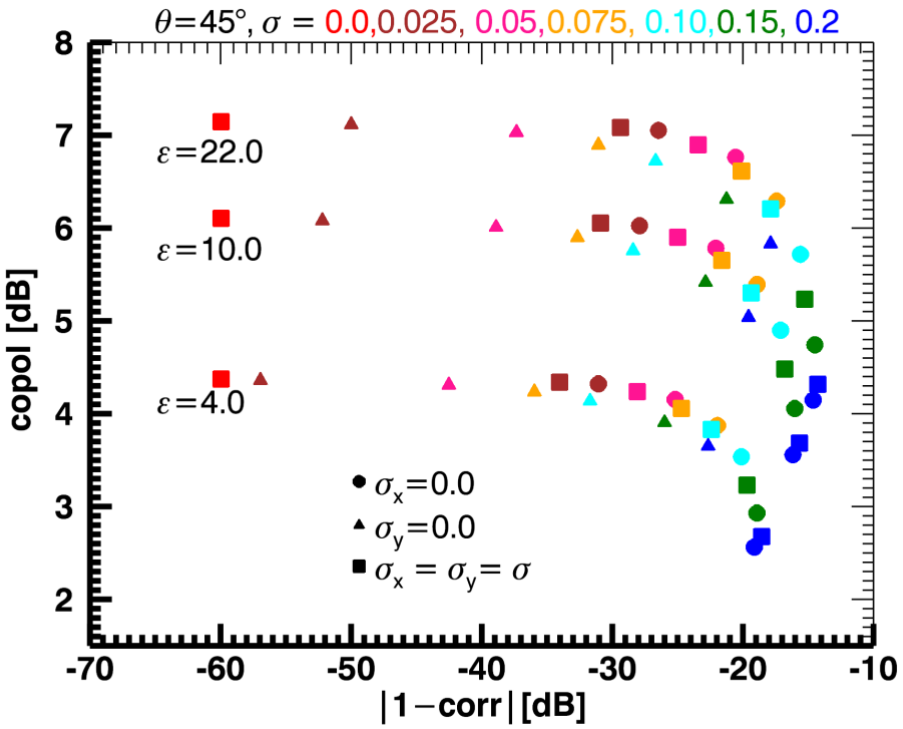

Use of ***copol-corr*** graphs should be preferred for bare soil moisture retrieval, whenever ***uncontrollable anisotropies*** may be present in the macroscopic roughness.

D. Simulation with a prescribed DEM: H and α decomposition

Lidar elevation Data (one meter resolution)

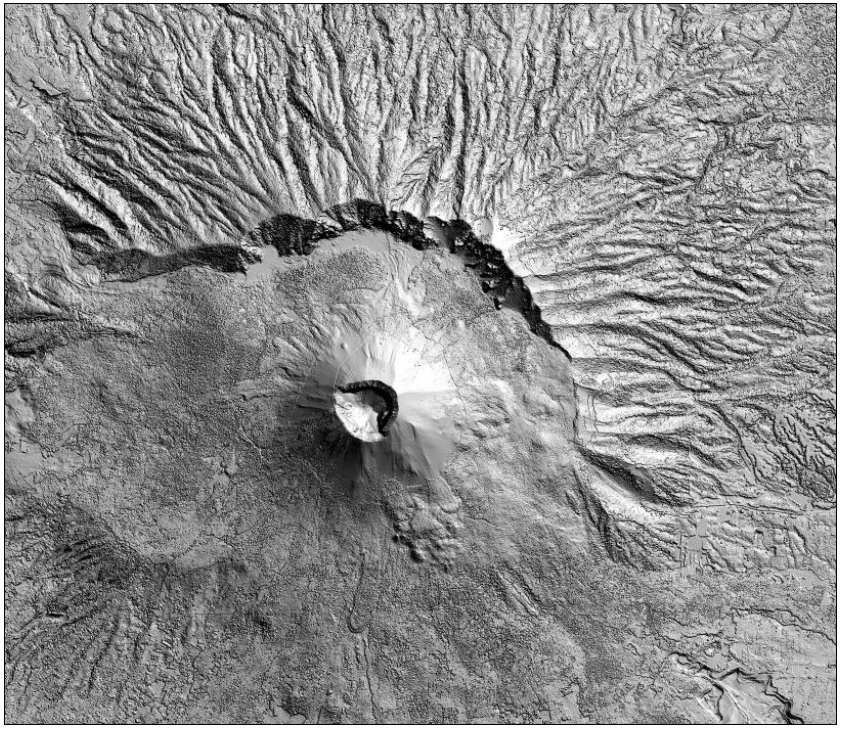

$$H = \sum_{i=1}^{3}(-P_i log_2 P_i)$$

$$P_i = \frac{\lambda_i}{\lambda_1+\lambda_2+\lambda_3}$$

$$H - \alpha$$

HH chanel

(a)

(b)

H is low and tend to be higher in low density

D. Simulation with a prescribed DEM:

Z9- Low entropy surface scattering: surfaces such as water at L and P-bands, sea ice at L-band, and very smooth land surfaces

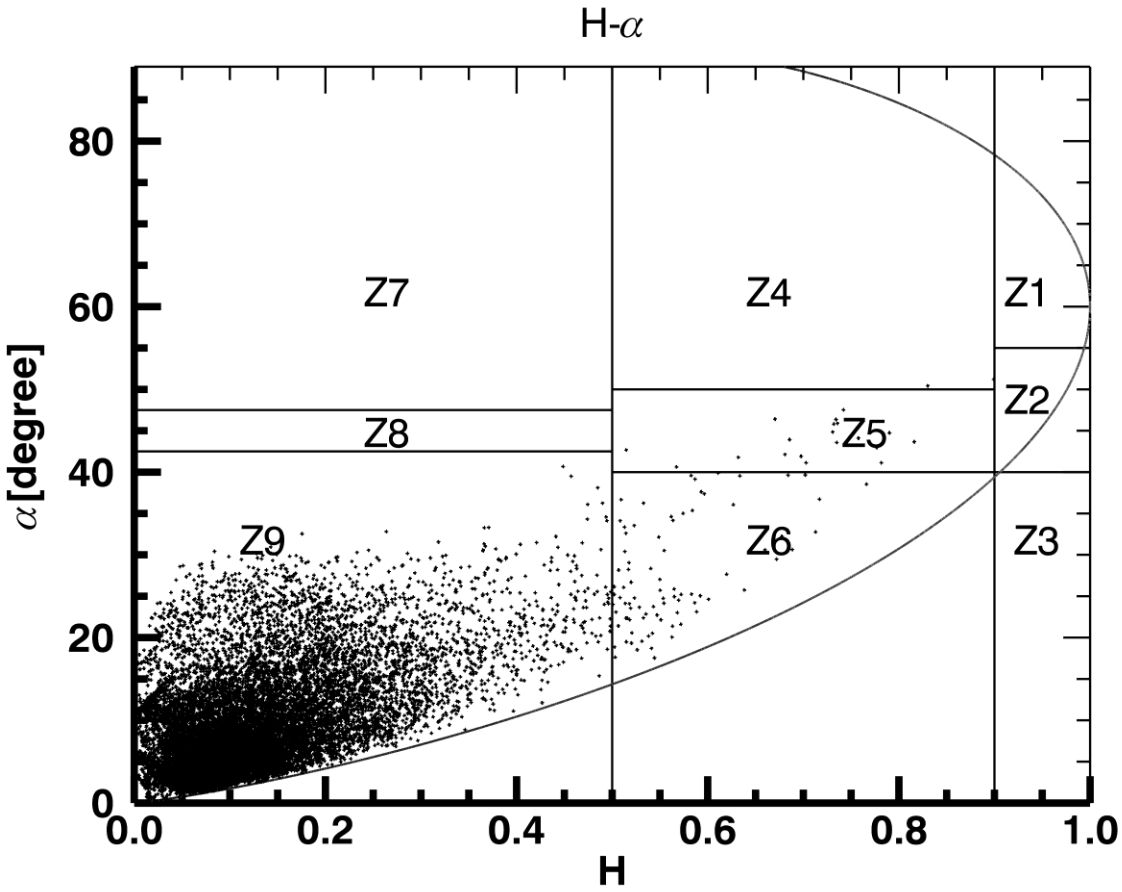

Scatterplot of the top images represented in the *H-α* plane partitioned according to the classification scheme.

E. Comparison with measured data (from University of Michigan-LCX POLARSCAT [5-6])

- Slightly rough bare soil surfaces 1 of [6]
- We fixed ε to the value measured in the top 4-cm soil layer
- Large-scale roughness, fixed in value to 0.17

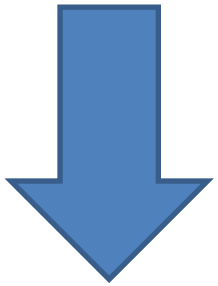

- At the most ***1dB*** (***0.4 dB***) for copol
- ***1.1dB*** for crosspol (wet) and a bit more for the dry case of 30° and comparibale to wet condition in higher look angles

Table 5.2. Comparision with measured data, surface 1-wet

surface 1-wet L-band (1.5 GHz) $\epsilon = 15.57$; $\sigma = 0.17$

θ (degrees)	*crosspol* (ground)	*copol* (ground)	*crosspol* (Pol-SARAS)	*copol* (Pol-SARAS)
30°	-21	2	-21.2	2.3
40°	-19	4	-20.1	3.6
50°	-20	6	-19.0	5.6
60°	-19	9	-18.1	8.2

Table 5.3. Comparision with measured data, surface 1-dry

surface 1-dry L-band (1.5 GHz) $\epsilon = 7.99$; $\sigma = 0.17$

θ (degrees)	*crosspol* (ground)	*copol* (ground)	*crosspol* (Pol-SARAS)	*copol* (Pol-SARAS)
30°	-19	1	-22.4	2.0
40°	-19	3	-21.3	3.1
50°	-20	4	-19.9	4.8
60°	-18	6	-19.0	6.9

[5] A. Iodice, A. Natale, and D. Riccio, "Retrieval of Soil Surface Parameters via a Polarimetric Two-Scale Model", IEEE Trans. Geosc. Remote Sens., vol. 49, no. 7, pp. 2531-2547, July 2011.
[6] Y. Oh, K. Sarabandi, and F. T. Ulaby, "An empirical model and an inversion technique for radar scattering from bare soil surfaces," IEEE Trans. Geosci. Remote Sens., vol. 30, no. 2, pp. 370381, Mar. 1992.

F. Directly compare simulated and real SAR polarimetric images - May 1998 NASA/JPL AIRSAR L-band polarimetric data of Camp Roberts, CA

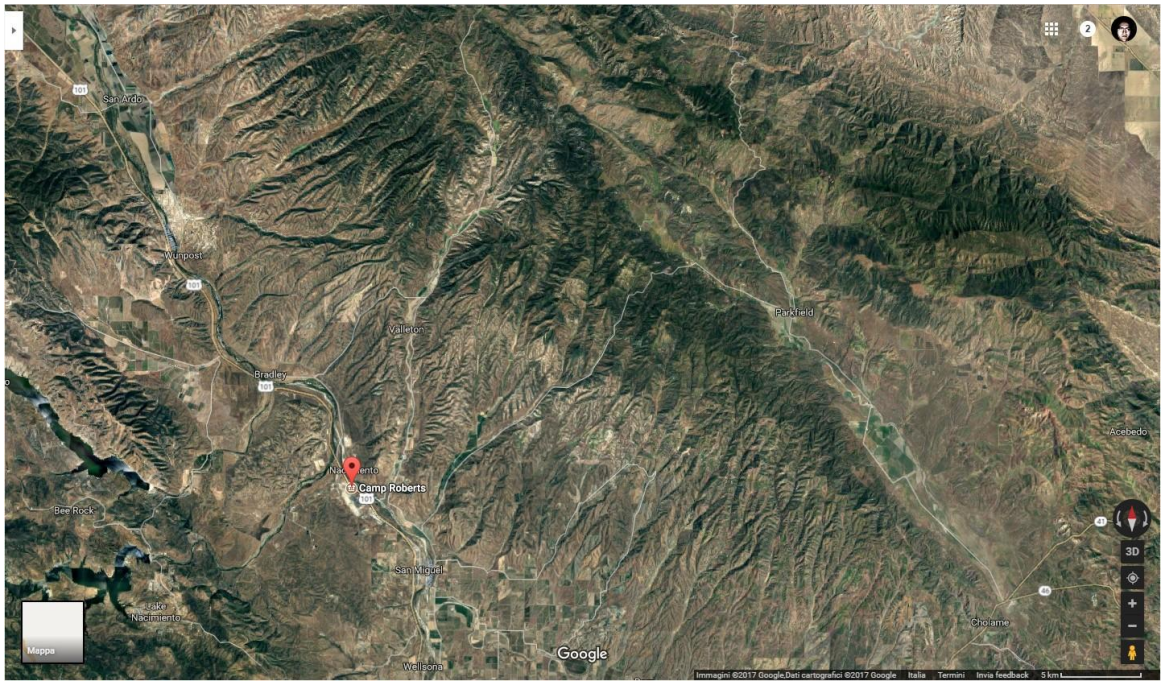

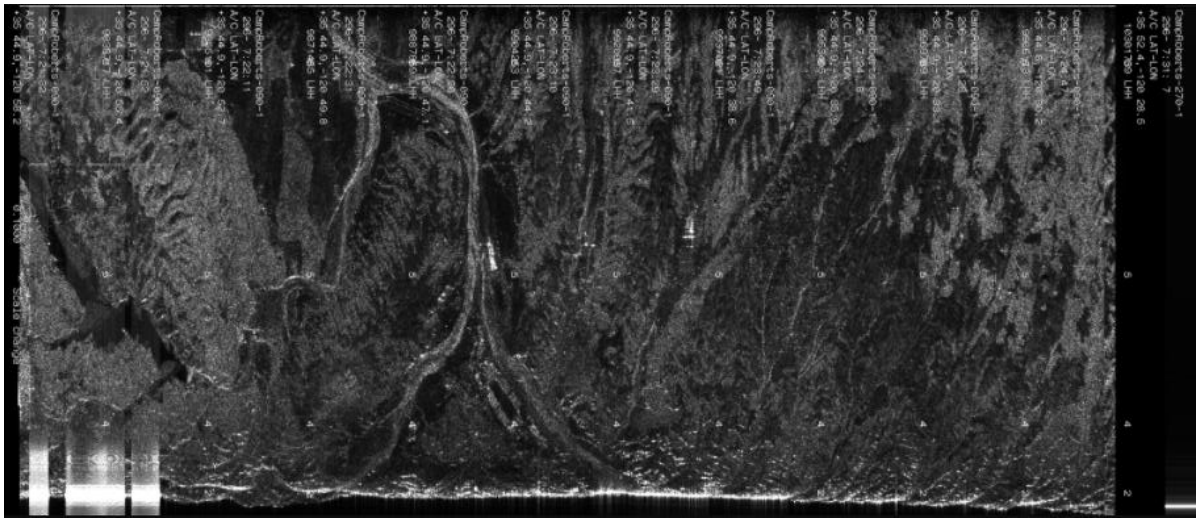

F. Directly compare simulated and real SAR polarimetric images - May 1998 NASA/JPL AIRSAR L-band polarimetric data of Camp Roberts, CA [7]

Sensor height	[km]	7.6813
Sensor velocity	[km/s]	0.4323
Look angle	[degree]	44.8
Azimuth antenna size	[m]	3
Range antenna size	[m]	0.8
Carrier frequency	[GHz]	1.2
Pulse duration	[μs]	10
Sampling rate	[MHz]	45
PRF	[Hz]	840.3
Doppler centroid	[Hz]	0
Chirp bandwidth	[MHz]	14
Topothesy	[m]	0.001
Hurst coefficient		0.8
Permittivity (ϵ)		22

(a)

(b)

$$I_2 = arctan\left(\frac{4Re\langle(i_{HH}-i_{VV})i_{HV}^*\rangle}{4\langle|i_{HV}|^2\rangle-\langle|i_{HH}-i_{VV}|^2\rangle}\right)$$

For bare soils, *only* depend on topography (β) [8]

$$R \Leftarrow \sqrt{\langle|i_{HH}-i_{VV}|^2\rangle/2}$$

$$G \Leftarrow \sqrt{2\langle|i_{HH}|^2\rangle}$$

$$B \Leftarrow \sqrt{\langle|i_{HH}-i_{VV}|^2\rangle/2}$$

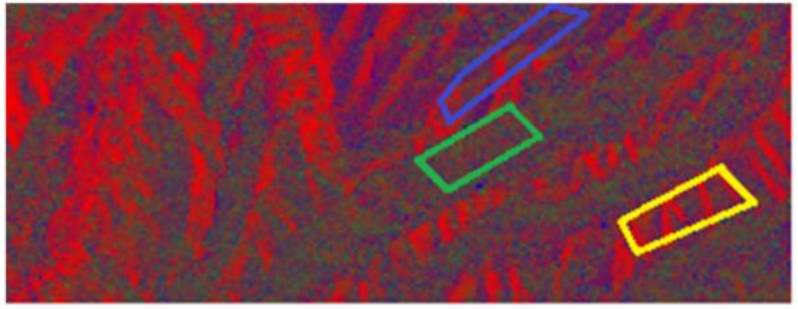

(c)

[7] Available online: https://airsar.jpl.nasa.gov/

[8] J.-S. Lee, D. L. Schuler, T. L. Ainsworth, E. Krogager, D. Kasilingam, and W. Boerner, "On the estimation of radar polarization orientation shifts induced by terrain slopes, IEEE Trans. Geosci. Remote Sens., vol. 40, no. 1, pp. 3041, 2002.

F. Directly compare simulated and real SAR polarimetric images - May 1998 NASA/JPL AIRSAR L-band polarimetric data of Camp Roberts, CA [7]

Histograms of real and simulated images for yellow region

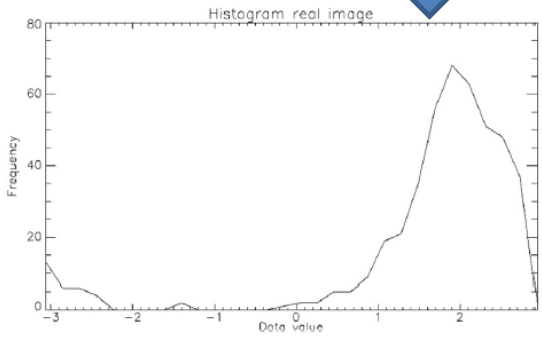

	YELLOW ROI		BLUE ROI		GREEN ROI	
	Mean value	Standard deviation	Mean value	Standard deviation	Mean value	Standard deviation
Actual SAR data	1.78	1.49	1.71	1.37	-0.89	1.86
Simulated $\sigma = 0.1$	1.87	1.07	1.90	1.07	-1.81	0.79
Simulated $\sigma = 0.15$	1.82	1.15	1.81	1.18	-1.76	0.86
Simulated $\sigma = 0.2$	1.62	1.36	1.64	1.39	-1.72	0.91

$$\sigma \uparrow \equiv \downarrow I_2$$

$$SD_{sm} < SD_{Re}$$

F. Directly compare simulated and real SAR polarimetric images - May 1998 NASA/JPL AIRSAR L-band polarimetric data of Camp Roberts, CA [7]

$I_2 \equiv 4\beta$ [8]

$\beta_{real} < \beta_{Dem}$

$\beta_{sim} < \beta_{Dem}$

	YELLOW ROI		BLUE ROI		GREEN ROI	
	No smoothing	2×2 smoothing	No smoothing	2×2 smoothing	No smoothing	2×2 smoothing
DEM	0.54	0.54	0.57	0.57	-0.54	-0.54
Actual SAR data	0.44	0.56	0.43	0.53	-0.22	-0.47
Simulated $\sigma = 0.025$	0.48	0.52	0.50	0.53	-0.46	-0.48
Simulated $\sigma = 0.1$	0.47	0.51	0.47	0.52	-0.45	-0.47
Simulated $\sigma = 0.2$	0.41	0.49	0.41	0.50	-0.43	-0.47
Simulated $\sigma_x = 0.2, \sigma_y = 0$	0.38	0.49	0.35	0.46	-0.41	-0.48
Simulated $\sigma_x = 0, \sigma_y = 0.2$	0.45	0.49	0.46	0.51	-0.43	-0.44

F. Directly compare simulated and real SAR polarimetric images - May 1998 NASA/JPL AIRSAR L-band polarimetric data of Camp Roberts, CA [7]

Smoothing with 2*2 boxcar:

✓Much better agreement with the DEM-derived ones
✓Effects of roughness, noise and vegetation are significantly reduced
✓Real and simulated data are in very good agreement

	YELLOW ROI		BLUE ROI		GREEN ROI	
	No smoothing	2×2 smoothing	No smoothing	2×2 smoothing	No smoothing	2×2 smoothing
DEM	0.54	0.54	0.57	0.57	-0.54	-0.54
Actual SAR data	0.44	0.56	0.43	0.53	-0.22	-0.47
Simulated $\sigma = 0.025$	0.48	0.52	0.50	0.53	-0.46	-0.48
Simulated $\sigma = 0.1$	0.47	0.51	0.47	0.52	-0.45	-0.47
Simulated $\sigma = 0.2$	0.41	0.49	0.41	0.50	-0.43	-0.47
Simulated $\sigma_x = 0.2, \sigma_y = 0$	0.38	0.49	0.35	0.46	-0.41	-0.48
Simulated $\sigma_x = 0, \sigma_y = 0.2$	0.45	0.49	0.46	0.51	-0.43	-0.44

Outline

PART I

- ✓ Railways' stabilities observed/modelled in Campania (Italy) by InSAR data
- ✓ Principles of InSAR and PSI
- ✓ Data, and data analysis
- ✓ Conclusions

PART II

- ✓ A fully polarimetric SAR raw signal simulator
- ✓ Polarimetirc simulation rationale
- ✓ Simulation results
- ✓ **Conclusions**

- **Pol-SARAS is based on the use of sound direct electromagnetic models.**
- **The simulated data of all the three polarization channels lead to correct/realistic covariance (or coherence) matrixes on the final images.**
- **Pol-SARAS accounts for only surface scattering contribution; however, volumetric and double-bounce contributions can be included, if reliable models are available.**
- **PTSM predictions are in good agreement with Pol-SARAS results.**
- **Our simulated data are in good agreement with the actual polarimetric data (from University of Michigan) for two different soil moisture conditions.**
- **Acceptable agreement with real SAR (AIRSAR) data has been observed, showing the potential of practical applications.**
- **Potential use in helping soil moisture, and/or orientation angle retrieval.**

Parts of this work have been published in the following journals/books:

D. Poreh, D. Riccio, "Building's subsidence observed in Mexico City by remote sensing data", Mapping urban areas from space conference, 4th November 2015, ESA Frascati.

D. Poreh, A. Iodice, D. Riccio, G. Ruello, "Railways' stabilities observed in Campania (Italy) by InSAR data", IEEE Young Professional, 4-6 December 2015, Barcelona.

G. Di Martino, A. Iodice, **D. Poreh** and D. Riccio, "Soil moisture retrieval from polarimetric SAR data: a short review of existing methods and a new one", European Space Agency, ESA SP 740 (Proceedings of Living Planet Symposium 2016), Prague (Czech Republic), May 2016, CD-ROM.

G. Di Martino, A. Iodice, **D. Poreh** and D. Riccio, "Polarimetric SAR Raw Signal Simulation", Proceedings RiNEM 2016, Parma (Italy), September 2016, in print.

G. Di Martino, A. Iodice, **D.Poreh**, D. Riccio, "A fully polarimetric SAR raw signal simulator", IEEE Young Professional, 20-21October 2016 DLR Germany.

G. Di Martino, A. Iodice, **D.Poreh**, D. Riccio, "Pol-SARAS: a fully polarimetric SAR raw signal simulator and its application to soil moisture retrieval", Pol-InSAR conference in Frascati 2017.

Parts of this work have been published in the following journals/books:

D. Poreh, A. Iodice, D. Riccio, G. Ruello, "Railways' stability observed in Campania (Italy) by InSAR data", European Journal of Remote Sensing, vol.49, pp. 417-431, 2016.

D. Amitrano, V. Belore, F. Cecinati, G. Di Martino, A. Iodice, P.-P. Mathieu, S. Medagli, **D. Poreh**, D. Riccio, G. Ruello, "Urban Areas Enhancement in Multitemporal SAR RGB Images Using Adaptive Coherence Window and Texture Information", IEEE Journal of Selected Topics in Applied Earth Observations and Remote Sensing, vol.9, no.8, pp. 3740-3752, 2016.

G. Di Martino, A. Iodice, **D.Poreh,** D. Riccio, "Pol-SARAS: a fully polarimetric SAR raw signal simulator for extended scenes", Under review for IEEE transaction papers.

G. Di Martino, A. Iodice, **D.Poreh**, D. Riccio, G. Ruello, "Physical models for evaluating the interferometric coherence of potential persistent scatterers", Proceedings on IGARSS 2017, Texas, USA.

G. Di Martino, A. Iodice, **D.Poreh**, D. Riccio, "A fully polarimetric SAR raw signal simulator", Proceedings on IGARSS 2017, Texas, USA.

D. Poreh, A. Iodice, D. Riccio, G. Ruello, "Railways' stability observation by satellite radar images", Book chapter in "Railway Engineering", InTECH, 2017.

Parts of this work have been published in the following journals/books:

Our work is also nominated to the Springer's thesis publication series, and is still under evaluation for printing (http://www.springer.com/series/8790).

Thank You for your attention

Any question or comment?

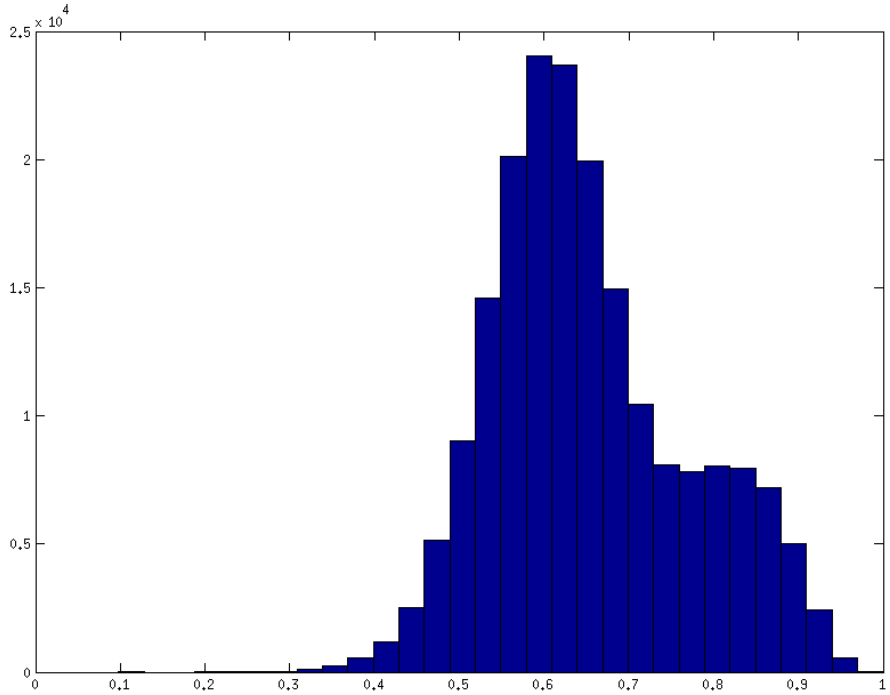

Coh

Linear

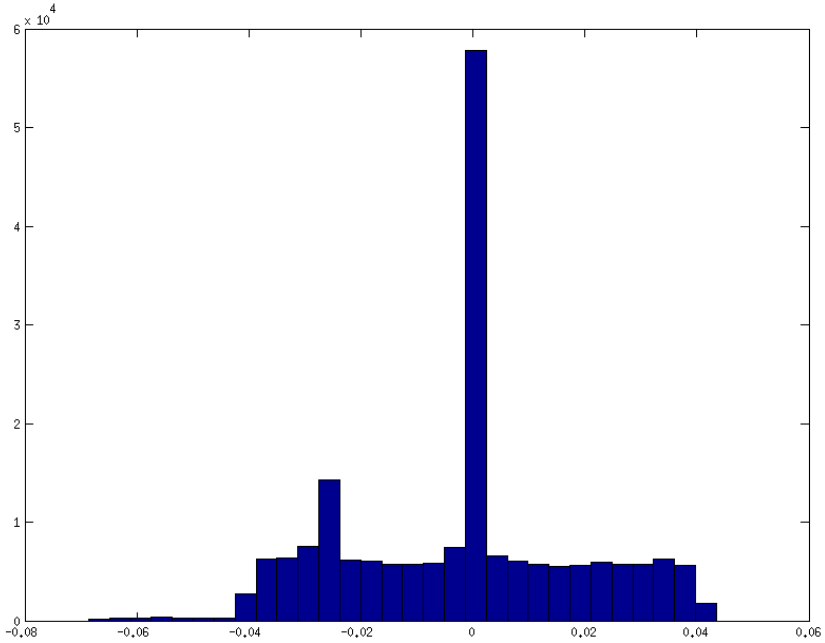

Approximate Cost

Satellite	Resolution	# Images	AOI (km^2)	Cost ($)
ERS	20x5	30	5 100 1000	25,000 40,000 75,000
Envisat	20x5	30	5 100 1000	32,000 50,000 100,000
Radarsat-1	20x5	30	5 100 1000	64,000 100,000 160,000
Radarsat-1	7x5	30	5 100 1000	72,000 115,000 185,000
TerraSAR-X Cosmo-SkyMed	3x3	30	5 100 1000	115,000 140,000 210,000

TABLE I
SIMULATION PARAMETERS

Sensor height	[km]	200
Sensor velocity	[km/s]	0.9
Azimuth antenna size	[m]	1.5
Range antenna size	[m]	8.5
Carrier frequency	[GHz]	1.28
Pulse duration	[μs]	1.9
Sampling rate	[MHz]	14
PRF	[Hz]	350
Doppler centroid	[Hz]	0
Chirp bandwidth	[MHz]	14
Topothesy	[m]	0.001
Hurst coefficient		0.8

$$\varphi_{ij}^{k} = -2\pi a_{ij}^{k} - \frac{4\pi}{\lambda} \cdot \frac{B_i^{\perp}}{R_i^m sin\theta_i^m} H_{ij} - \frac{4\pi}{\lambda} D_{ij} + \frac{4\pi}{\lambda} \cdot \frac{B_i^{\perp}}{R_i^m tan\theta_i^m} \eta_{ij}^{m} + \frac{2\pi}{\upsilon}(f_{dc,i}^{m} - f_{dc,i}^{s})\xi_{ij}^{m}$$

$$+\mathrm{f}_{\varphi_{orbit}}(\xi_{ij}^{m} - \eta_{ij}^{m}) + \varphi_{ijatmo}^{k} + n_{ij}^{k},$$

where:

φ_{ij}^{k}	double-difference phase observation,
$B_i^{\perp}$, R_i^m,θ_i^m	perpendicular baseline, range and incidence angle for PS i,
a_{ij}^{k}	integer ambiguity between PS i and PS j,
H_{ij}^{k}	(residual) topographic height between PS i and PS j,
D_{ij}^{k}	deformation between PS i and PS j,
ξ_{ij}^{m}	sub-pixel position in azimuth direction,
η_{ij}^{m}	slant-range sub-pixel position,
η, ξ	range and azimuth radar coordinates,
υ	satellite velocity,
$f_{dc,i}^{m}$, $f_{dc,i}^{s}$	Doppler centroid frequency of master and slave acquisition,
$f_{\varphi orbit}(\xi_{ij}^{m} - \eta_{ij}^{m})$	(residual) orbital trend as a function of radar coordinates,
φ_{ijatmo}^{k}	(residual) atmospheric signal,
n_{ij}^{k}	measurement noise.

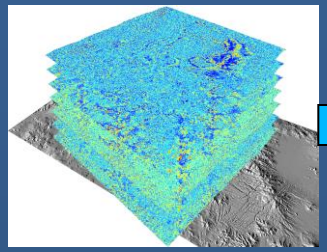

IFGs

PSC1

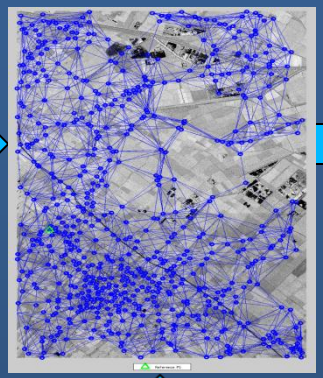

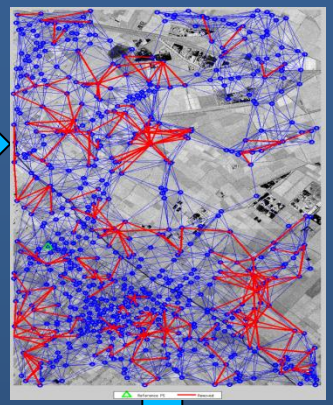

Phase unwrapping

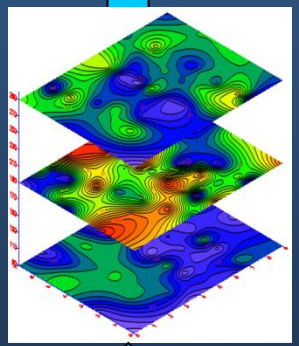

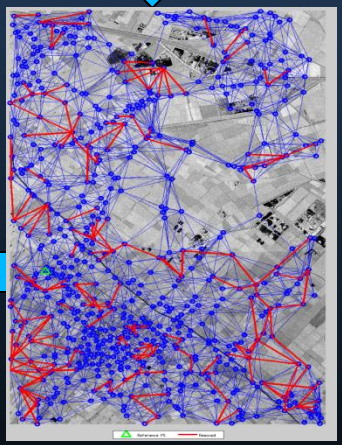

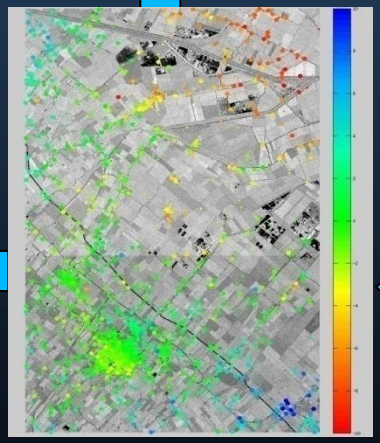

APS filtering

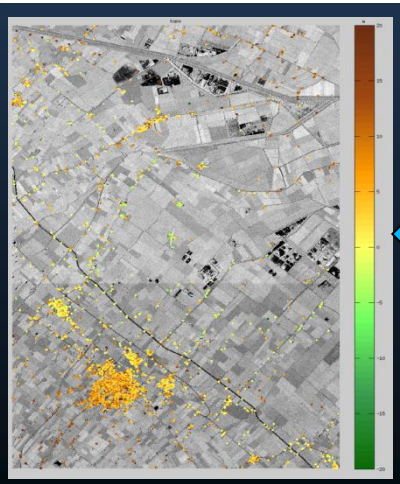

PS's height

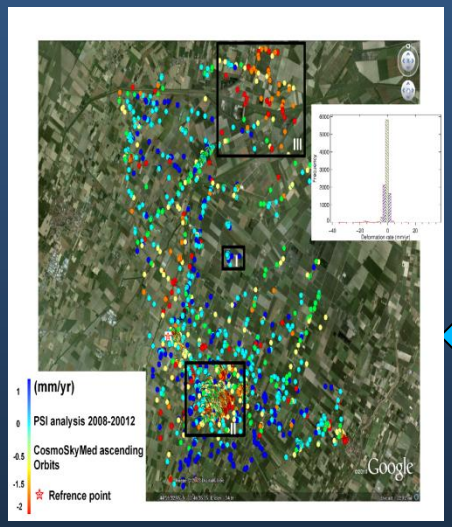

PS

Laser Profiler

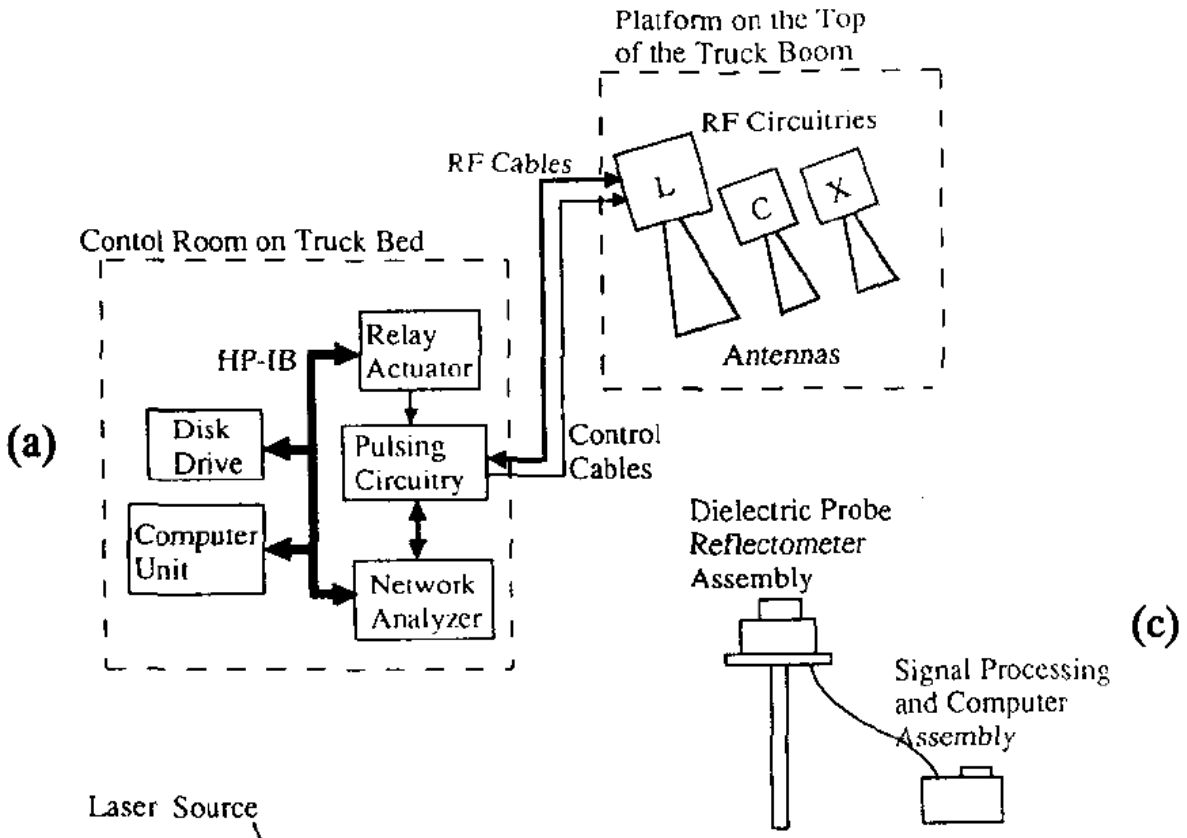

[6] Y. Oh, K. Sarabandi, and F. T. Ulaby, "An empirical model and an inversion technique for radar scattering from bare soil surfaces," IEEE Trans. Geosci. Remote Sens., vol. 30, no. 2, pp. 370381, Mar. 1992.

• **Same realization of random variable in Small Perturbation Method (SPM) or the Physical Optics (PO) regimes, in such a way to guarantee that three polarimetric channels are <u>not independent</u>. However, the facet slopes' randomness, ensures <u>de-correlation</u> among the three polarimetirc channels**

$$\gamma_{pq}(x, r; \vartheta_l, \beta, \epsilon) = \chi_{pq}(x, r, \vartheta_l, \beta, \epsilon) w(x, r; \vartheta_l)$$

$$\underline{\underline{\chi}}(\vartheta_l, \beta, \epsilon) = \underline{\underline{R}}_2(\beta) \begin{pmatrix} F_H(\vartheta_l, \epsilon) & 0 \\ 0 & F_V(\vartheta_l, \epsilon) \end{pmatrix} \underline{\underline{R}}_2^{-1}(\beta)$$

• **In the SPM case :**

$$\langle |w(\vartheta_l)|^2 \rangle = k^4 cos^4 \vartheta_l W(2k sin \vartheta_l)$$

$$W(k) = S_0 k^{-2-2H_t}$$

A stochastic process (*fBm*) for small-scale roughness modeling